





# Metatranscriptomic Sequencing Reveals Host Species as an Important Factor Shaping the Mosquito Virome

Cixiu Li,<sup>a,b</sup> Shuqi Liu,<sup>a,b</sup> Hong Zhou,<sup>a,b</sup> Wei Zhu,<sup>a,b</sup> Mingxue Cui,<sup>a,b</sup> Juan Li,<sup>a,b</sup> Jiao Wang,<sup>c</sup> Jiangyun Liu,<sup>c</sup> Jin Zhu,<sup>d</sup> Weiping Li,<sup>d</sup> Yuhai Bi,<sup>e</sup>  
 Michael J. Carr,<sup>f,g</sup>  Edward C. Holmes,<sup>h</sup>  Weifeng Shi<sup>b,i</sup>

<sup>a</sup>Department of Pathogen Biology, School of Clinical and Basic Medicine, Shandong First Medical University & Shandong Academy of Medical Sciences, Ji'nan, China

<sup>b</sup>Key Laboratory of Emerging Infectious Diseases in Universities of Shandong, Shandong First Medical University & Shandong Academy of Medical Sciences, Taian, China

<sup>c</sup>Mengla County Center for Disease Control and Prevention, Mengla, China

<sup>d</sup>Xishuangbanna Prefecture Center for Disease Control and Prevention, Jinghong, China

<sup>e</sup>Key Laboratory of Pathogenic Microbiology and Immunology, Institute of Microbiology, Chinese Academy of Sciences, Beijing, China

<sup>f</sup>National Virus Reference Laboratory, School of Medicine, University College Dublin, Dublin, Ireland

<sup>g</sup>International Collaboration Unit, International Institute for Zoonosis Control, Hokkaido University, Sapporo, Japan

<sup>h</sup>Sydney Institute for Infectious Diseases, School of Medical Sciences, The University of Sydney, Sydney, New South Wales, Australia

<sup>i</sup>School of Public Health, Shandong First Medical University & Shandong Academy of Medical Sciences, Ji'nan, China

**ABSTRACT** Mosquitoes are important vector hosts for numerous viral pathogens and harbor a large number of mosquito-specific viruses as well as human-infecting viruses. Previous studies have mainly focused on the discovery of mosquito viruses, and our understanding of major ecological factors associated with virome structure in mosquitoes remains limited. We utilized metatranscriptomic sequencing to characterize the viromes of five mosquito species sampled across eight locations in Yunnan Province, China. This revealed the presence of 52 viral species, of which 19 were novel, belonging to 15 viral families/clades. Of particular note was *Culex* hepacivirus 1, clustering within the avian clade of hepaciviruses. Notably, both the viromic diversity and abundance of *Aedes* genus mosquitoes were significantly higher than those of the *Culex* genus, while *Aedes albopictus* mosquitoes harbored a higher diversity than *Aedes aegypti* mosquitoes. Our findings thus point to discernible differences in viromic structure between mosquito genera and even between mosquito species within the same genus. Importantly, such differences were not attributable to differences in sampling between geographical location. Our study also revealed the ubiquitous presence of the endosymbiont bacterium *Wolbachia*, with the genetic diversity and abundance also varying between mosquito species. In conclusion, our results suggested that the mosquito host species play an important role in shaping the virome's structure.

**IMPORTANCE** This study revealed the huge capability of mosquitoes in harboring a rich diversity of RNA viruses, although relevant studies have characterized the intensively unparalleled diversity of RNA viruses previously. Furthermore, our findings showed discernible differences not only in viromic structure between mosquito genera and even between mosquito species within the same genus but also in the genetic diversity and abundance of *Wolbachia* between different mosquito populations. These findings emphasize the importance of host genetic background in shaping the virome composition of mosquitoes.

**KEYWORDS** mosquito, virome, evolution, ecology, metatranscriptomics

Numerous mosquito-borne viruses are able to cause disease in humans and other vertebrates, with the potential for major epidemics and pandemics that disrupt global public health and threaten human and animal populations (1, 2). With the deployment of next-generation sequencing, particularly metatranscriptomics (total RNA sequencing), an enormous genetic diversity of viruses in mosquitoes has been identified (3, 4), the majority of

**Editor** Biao He, Changchun Veterinary Research Institute

**Copyright** © 2023 Li et al. This is an open-access article distributed under the terms of the [Creative Commons Attribution 4.0 International license](https://creativecommons.org/licenses/by/4.0/).

Address correspondence to Weifeng Shi, shiwf@ioz.ac.cn.

The authors declare no conflict of interest.

**Received** 15 November 2022

**Accepted** 18 January 2023

**Published** 14 February 2023

which are insect specific (5, 6) and are distinct from viruses of medical importance. As such, the presence of disease-causing viruses in mosquitoes is probably the exception rather than the rule. However, how ecological factors impact the composition and diversity of mosquito viromes remains unclear (3, 7), limiting our understanding of the ecological drivers of host-switching and spillover events and their public health risks (8). In addition, the pathogenicity of most mosquito-borne viruses is poorly understood, even though some may pose a risk to public health or modulate the transmission of pathogenic viruses (9).

Jinghong City, part of the Xishuangbanna Dai Autonomous Prefecture of Yunnan Province, is located on the southern border of China and geographically adjacent to Laos, Myanmar, and Vietnam, where some tropical viral infectious diseases are endemic (10, 11). In recent years, mosquito-associated infectious diseases, such as dengue fever and Japanese encephalitis (12, 13), have been imported into Xishuangbanna. In addition, the stable tropical climate in Xishuangbanna facilitates mosquito breeding and production (10), constituting an important driver of infectious disease outbreaks. Indeed, several large-scale dengue outbreaks have been reported in Xishuangbanna since the first documented epidemic there in 2013 (12, 14, 15). Therefore, characterization of the virus spectrum in the key mosquito species (particularly species from the *Aedes* and *Culex* genera that are known to harbor pathogenic viruses responsible for epidemics in human and animal populations) and identification of possible associations between mosquito species and virome structures are of vital importance to prevent and control future tropical disease outbreaks here and potentially elsewhere.

Herein, we characterized the total transcriptomes of 56 mosquito pools, comprising 991 mosquitoes from five invertebrate species collected from eight locations in Jinghong, Xishuangbanna. We analyzed the genetic diversity of RNA viruses in these mosquito species and identified the complete coding sequences of 52 RNA viruses, including 19 previously undescribed viruses. We further determined the evolutionary relationships of the novel viruses identified here and revealed an association between mosquito vector species and virome structure by comparing the compositions and structures of the viral communities within different hosts.

## RESULTS

**The mosquito viromes.** A total of 991 mosquitoes were collected in 2018 from eight locations (A to H) in Jinghong City, Yunnan Province, China (Fig. 1A; see Table S1 in the supplemental material). The mosquitoes comprised five species: *Culex quinquefasciatus* ( $n = 425$ ), *Aedes aegypti* ( $n = 355$ ), *Aedes albopictus* ( $n = 179$ ), *Lutzia halifaxii* ( $n = 10$ ), and *Armigeres subalbatus* ( $n = 22$ ) (Fig. 1B; Table S1). Samples were pooled into 56 libraries based on mosquito species and collection location (Table S1). Metatranscriptomic sequencing generated between 34,777,328 and 192,424,498 reads per library (Table S1).

Subsequent analyses revealed the complete coding sequences of 52 RNA viruses, 19 of which were novel viruses due to a sequence similarity of  $<90\%$  in the RNA-dependent RNA polymerase (RdRp) protein (Table 1). All viruses fell within known viral families or orders: *Chrysoviridae* ( $n = 1$ ), *Partitiviridae* ( $n = 5$ ), *Reoviridae* ( $n = 1$ ), *Totiviridae* ( $n = 3$ ), *Bunyavirales* ( $n = 7$ ), *Mononegavirales* ( $n = 9$ ), *Orthomyxoviridae* ( $n = 6$ ), *Flaviviridae* ( $n = 3$ ), *Namaviridae* ( $n = 3$ ), *Negevirus* ( $n = 2$ ), *Solemoviridae* ( $n = 6$ ), *Tombusviridae* ( $n = 1$ ), *Tymoviridae* ( $n = 2$ ), *Virgaviridae* ( $n = 2$ ), and *Permutotetraviridae* ( $n = 1$ ) (Table 1).

For each library, the number of virus species varied from 2 to 16, with the exception of one *C. quinquefasciatus* library from location H, in which no viruses were detected (Fig. 1C). The abundance of each virus varied from 2.00 to 6,825.80 reads mapped per million input reads (RPM) across the pools (Fig. 1D; Table S2). In comparison, the abundance of the mosquito host, determined by *COI* gene sequencing, varied between 1.30 and 774.92 RPM (Fig. 1D; Table S1). A total of 14 viruses, including 2 of *Partitiviridae* (*Aedes partiti*-like virus 1 [AePLV1], and *Aedes partiti*-like virus 2), 1 of *Reoviridae* (*Aedes reo*-like virus 1 [AeRLV1]), 1 *Bunyavirales* (Phasi Charoen-like phasivirus), 2 of *Mononegavirales* (*Aedes albopictus* anphevirus and *Culex quinquefasciatus* rhabdo-like virus 1), 2 of *Orthomyxoviridae*

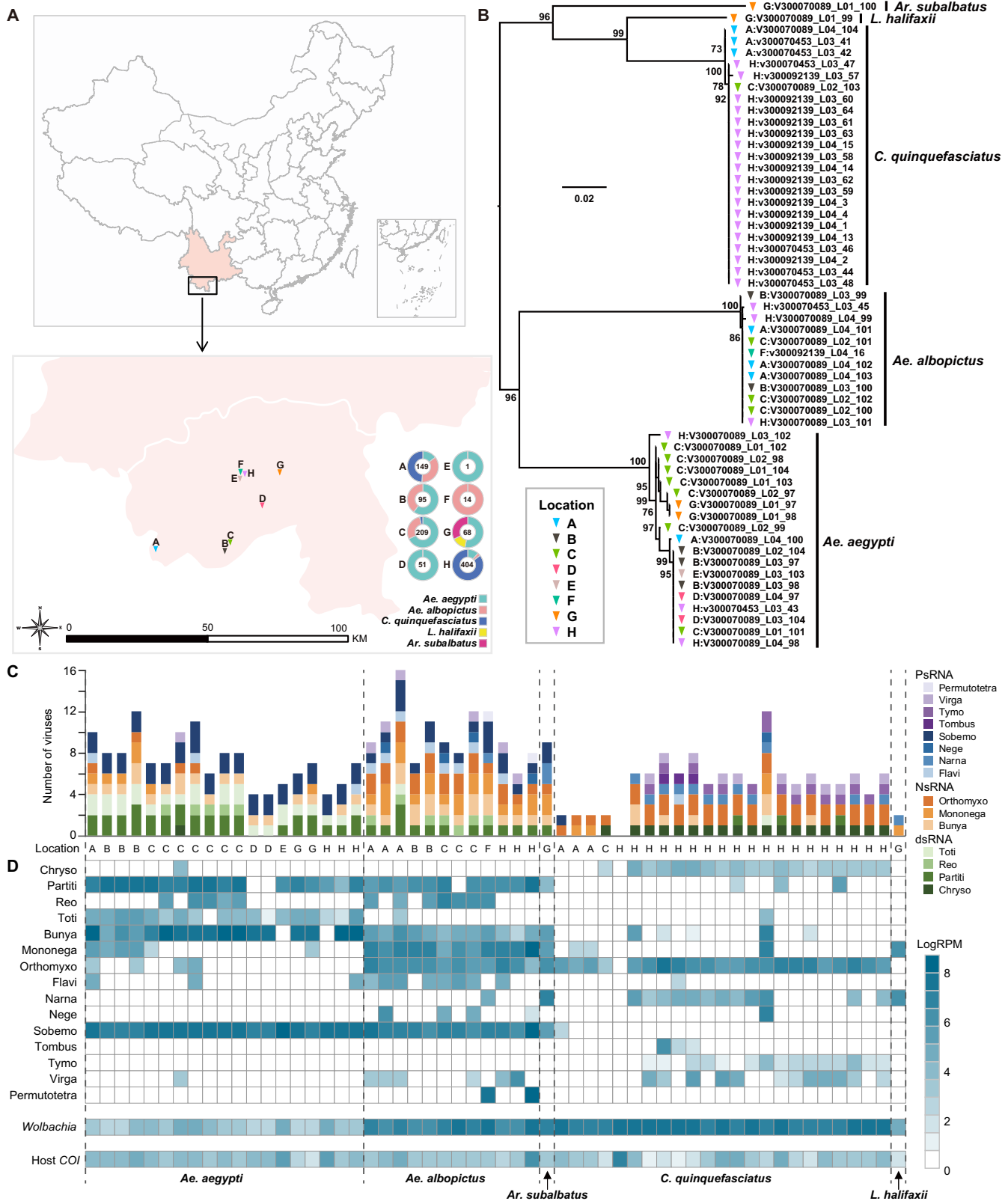


**FIG 1** Geographic locations and the species of the mosquito samples and overview of the RNA viruses and the *Wolbachia* bacteria identified in this study. (A) Sampling sites in Jinghong City and the mosquito species composition of each site. The mosquito species and the number of mosquitoes are shown in different colors. The maps were first created using ArcMap v10.4.1 and further edited using Adobe Illustrator 2020. (B) Species identification was based on phylogenetic analysis of the cytochrome c oxidase (COI) gene of the mosquitoes. (C) Number of viral species identified in each library, colored by virus type; (D) heat map showing the abundance (measured by RPM) of microbial species and the host COI gene in each of the 56 pools sequenced here.

**TABLE 1** Mosquito RNA viruses discovered in this study

Virus no.	Classification	Virus name <sup>a</sup>	Segment no.	Length (nt)	Closest relative	RdRp aa identity (%)	RPM <sup>b</sup>
<b>dsRNA viruses</b>							
1	Chrysoviridae related	Shuangao chryso-like virus 1 YN2018	4		Shuangao chryso-like virus 1 strain mosWSB68555	100	140
2	Partitiviridae related	Aedes partiti-like virus 1 YN2018	2		Aedes partiti-like virus 1 isolate Jane	100	2,539
3	Partitiviridae related	Aedes partiti-like virus 2*	1	1,709	Culex tritaeniorhynchus partitivirus 17CxlTNGK-Ctr	61.17	1,770
4	Partitiviridae related	Armigeres partiti-like virus 1*	1	1,486	Aedes partiti-like virus 1 isolate Jane	83.47	57
5	Partitiviridae related	Sonbo virus YN2018	3		Sonbo virus isolate OTU64	99.46	179
6	Partitiviridae related	Veradero virus YN2018	2		Veradero virus isolate Vv.Pozarica20	99.62	663
7	Reoviridae related	Aedes reo-like virus 1*	2	4,216/3,096	Shenzhen reo-like virus 2	30.00	922
8	Totiviridae related	Aedes aegypti toti-like virus YN2018	1		Aedes aegypti toti-like virus strain 2017-PB-AAM-5	98.70	32
9	Totiviridae related	Aedes aegypti totivirus YN2018	1		Aedes aegypti totivirus GH115	97.16	289
10	Totiviridae related	Culex toti-like virus 1*	1	7,194	Fitzroy Crossing toti-like virus 2 isolate FCToLV2/pool-7	73.20	81
<b>-ssRNA viruses</b>							
11	Bunyavirales	Aedes bunya-like virus 1*	1	7,731	Salavivirus Mos8CM0	48.54	196
12	Bunyavirales	Barstukas virus YN2018	3		Barstukas virus isolate CMS002_026c_WVAL	99.54	146
13	Bunyavirales	Culex bunyavirus 1 YN2018	1		Bunyavirales sp. strain YX392	96.06	683
14	Bunyavirales	Culex quinquefasciatus bunyavirus 1*	3	7,102/3,676/1,642	Qingnian mosquito virus strain YC179	88.78	271
15	Bunyavirales	Culex phasma-like virus YN2018	3		Culex phasma-like virus strain mos191gb30698	99.91	627
16	Bunyavirales	Phasi Charoen-like phasivirus YN2018	3		Phasi Charoen-like phasivirus strain Zhanjiang01	99.28	4,271
17	Bunyavirales	Zhee mosquito virus YN2018	1		Zhee mosquito virus strain XC1-8	99.22	196
18	Mononegavirales	Aedes rhabdovirus 1*	1	10,320	Merida virus isolate CC_H	48.08	21
19	Mononegavirales	Aedes albopictus anphevirus YN2018	1		Aedes albopictus anphevirus strain USA	99.46	5,462
20	Mononegavirales	Aedes anphevirus YN2018	1		Aedes anphevirus isolate Nakhon Nayok	99.71	344
21	Mononegavirales	Armigeres rhabdo-like virus 2*	1	10,143	San Gabriel mononegavirus isolate San Gabriel Valley	52.71	37
22	Mononegavirales	Armigeres rhabdo-like virus 1*	1	12,152	Formosus virus isolate U30	72.52	169
23	Mononegavirales	Culex rhabdo-like virus 2*	1	11,680	Culex rhabdo-like virus strain CRVL/Los Angeles	73.38	637
24	Mononegavirales	Culex mononega-like virus 2 YN2018	1		Culex mononega-like virus 2 strain mos191X56446	99.76	26
25	Mononegavirales	Culex quinquefasciatus rhabdo-like virus 1	1	11,508	Culex pseudovishnui rhabdo-like virus 17NGK-Cps-217	94.67	1,149
26	Mononegavirales	San Gabriel mononegavirus YN2018	1		San Gabriel mononegavirus isolate San Gabriel Valley	98.67	93
27	Orthomyxoviridae related	Aedes orthomyxo-like virus 2 YN2018	4		Aedes orthomyxo-like virus 2 isolate Italy Rome	99.35	409
28	Orthomyxoviridae related	Armigeres orthomyxo-like virus 1*	5	2,437/2,425/2,218/1,835/1,509	Usinis virus isolate CMS002_026e_WVAL	69.27	437
29	Orthomyxoviridae related	Wuhan mosquito virus 6 YN2018	6		Wuhan mosquito virus 6 strain YX592	100	1,659
30	Orthomyxoviridae related	Guadeloupe mosquito quaranja-like virus 1 YN2018	7		Guadeloupe mosquito quaranja-like virus 1 isolate CMS002_017a_SAND	99.35	25

(Continued on next page)

TABLE 1 (Continued)

Viruses no.	Classification	Viruses name <sup>a</sup>	Segment no.	Length (nt)	Closest relative	RdRp aa identity (%)	RPM <sup>b</sup>
31	Orthomyxoviridae related	Usinis virus YN2018	8		Usinis virus isolate CMS002_026e_WVAL	99.62	820
32	Orthomyxoviridae related	Wuhan mosquito virus 4 YN2018	5		Wuhan mosquito virus 4 strain XC3-4	100	565
+ssRNA viruses							
33	Flaviviridae related	Aedes flavivirus YN2018	1		Aedes flavivirus strain Bangkok	99.67	287
34	Flaviviridae related	Cell fusing agent virus YN2018	1		Cell fusing agent virus isolate KPP	99.19	107
35	Flaviviridae related	Culex hepacivirus 1*	1	8,997	Jogalong virus isolate P1-10	54.38	11
36	Narnaviridae related	Zhejiang mosquito virus 3 YN2018	1		Zhejiang mosquito virus 3 strain moshB236413	95.23	485
37	Narnaviridae related	Hubei mosquito virus 3 YN2018	1		Hubei mosquito virus 3 strain 3mos6141	98.2	806
38	Narnaviridae related	Mosquito narna-like virus 1*	1	3,160	Ochlerotatus-associated narna-like virus 2 isolate acc_9.11s	36.17	114
39	Negevirus related	Aedes albopictus negev-like virus YN2018	1		Aedes albopictus negev-like virus isolate Aag2.wAlbB	99.12	399
40	Negevirus related	Culex quinquefasciatus negev-like virus 1*	1	10,894	Parry's Creek negev-like virus 1 isolate PCNLV1/pool-12	90.05	1,132
41	Solemoviridae related	Aedes sobemo-like virus 1*	1	2,782	Hubei sobemo-like virus 41 strain spider133517	87.6	11
42	Solemoviridae related	Guadeloupe mosquito virus YN2018	2		Guadeloupe mosquito virus isolate CMS002_019a_SAND	99.55	3,013
43	Solemoviridae related	Guangzhou sobemo-like virus YN2018	2		Guangzhou sobemo-like virus strain 18-GZ-adult	99.77	5,457
44	Solemoviridae related	Hubei sobemo-like virus 41 YN2018	1		Hubei sobemo-like virus 41 strain spider133517	99.19	4
45	Solemoviridae related	Humaita Tubiacanga virus YN2018	2		Humaita-Tubiaccanga virus strain Ab-AAF	99.21	1,572
46	Solemoviridae related	Mosquito sobemo-like virus 1*	2	3,055/1,626	Guadeloupe mosquito virus isolate CMS002_019a_SAND	83.45	296
47	Tombusviridae related	Culex tomlus-like virus 1*	1	3,776	Dansoman virus strain INNplus3391	48.81	385
48	Tymoviridae related	Culex quinquefasciatus tymo-like virus 1*	1	7,859	Culex pseudovishnui tymo-like virus 17CxNGK-Cps2-1535	87.01	58
49	Tymoviridae related	Guadeloupe Culex tymo-like virus YN2018	1		Guadeloupe Culex tymo-like virus isolate CMS002_022a_SAND	96.74	47
50	Virgaviridae related	Aedes binegev-like virus 2 YN2018	2		Aedes binegev-like virus 2 isolate Shenzhen	99.79	387
51	Virgaviridae related	Hubei virga-like virus 2 YN2018	1		Hubei virga-like virus 2 isolate CMS001_019_ALCO	98.37	328
52	Permutotetraviridae related	Sarawak virus YN2018	1		Sarawak virus strain SWK-M26	97.23	6,826

<sup>a</sup>Asterisks indicate novel viruses identified in this study.

<sup>b</sup>RPM, reads per million. The largest one is shown if detected in multiple libraries.

(Wuhan Mosquito Virus 6 and Usinis virus), 1 of *Narnaviridae* (Hubei mosquito virus 3), 1 of *Negevirus* (*Culex quinquefasciatus* negev-like virus 1), 3 of *Solemoviridae* (Guadeloupe mosquito virus, Guangzhou sobemo-like virus, and Humaita Tubiacanga virus), and 1 of *Permutotetraviridae* (Sarawak virus) (Fig. 1D; Table S2), were more abundant than the host *COI* gene (with the highest abundance at 774.92 RPM) (Table S2).

**Phylogenetic relationships and viral genome characterization. (i) Double-stranded RNA viruses.** We identified 10 double-stranded RNA (dsRNA) viruses belonging to *Chrysoviridae* ( $n = 1$ ), *Partitiviridae* ( $n = 5$ ), *Reoviridae* ( $n = 1$ ), and *Totiviridae* ( $n = 3$ ). With the exception of *Aedes* reo-like virus 1 from *Reoviridae*, the other nine viruses were related to those previously identified in mosquitoes (Fig. 2).

Two novel ArPLV1 and AePLV2 viruses clustered with uncharacterized partiti-like viruses identified from different mosquito genera (Fig. 2A), thereby expanding the known host range of partiti-like viruses. The single-gene segments of both viruses contained a single open reading frame (ORF) sharing 83.47% and 61.17% amino acid similarity with their closest relatives, respectively (Table 1). Like other totiviruses, the *Culex* toti-like virus 1 (CTLV1) identified in the present study possessed an unsegmented genome comprising two major ORFs (Fig. 2B). CTLV1 clustered with unclassified toti-like viruses also from *Culex* mosquitoes and shared 73.20% amino acid similarity with its closest relative (Table 1). Finally, the only novel reovirus identified here, *Aedes* reo-like virus 1 (AeRLV1), comprised two segments containing three ORFs and was most closely related to Shenzhen reo-like virus 2 from *Tyrophagus* (Fig. 2D). AeRLV1 shared only 30% amino acid similarity over the conserved RdRp region (Table 1) and formed a distant clade with viruses identified from the class *Arachnoidea* (Fig. 2D).

**(ii) Negative-sense, single-stranded RNA viruses.** Twenty-two negative-sense, single-stranded RNA (–ssRNA) viruses with complete coding regions were identified in this study: 7 fell within the order *Bunyavirales*, 9 fell within the order *Mononegavirales*, and the remaining 6 belonged to the family *Orthomyxoviridae* and a related clade (Fig. 3).

Five of the seven *Bunyavirales* viruses were related to previously described mosquito viruses, with 96 to 100% amino acid identities to their closest relatives, including two *Phasmaviridae* viruses and three *Phenuiviridae* viruses (Fig. 3A). Although *Culex quinquefasciatus* bunyavirus 1 (CQBV1) fell within the *Bunyavirales* and shared 88.78% amino acid similarity to the most closely related virus (Qingnian mosquito virus [QMV]) (4), both CQBV1 and QMV diverged extremely from previously described viruses and formed a distinct lineage within the *Bunyavirales* (Fig. 3A), exhibiting less than 23% amino acid similarity over the RdRp protein. Similar to the typical genomic structure of the order *Bunyavirales*, the two viruses contained three gene segments. Hence, CQBV1 and QMV may represent a putative new family of the *Bunyavirales* (Fig. 3A). Another novel bunyavirus, *Aedes* bunya-like virus 1 (ABLV1), identified here also contained three gene segments and fell within the *Phenuiviridae* (Fig. 3A). ABLV1 clustered with reference strains identified in various mosquitoes, exhibiting 48.54% amino acid similarity to the most closely related virus (*Salarivirus*) (Fig. 3A).

We identified five novel viruses clustering within the *Rhabdoviridae*, four of which fell within the subfamily *Alpharhabdovirinae* and one belonging to the *Betarhabdovirinae* (Fig. 3B). *Armigeres* rhabdo-like virus 2 (ARLV2) was identified in *Armigeres* mosquitoes and was closely related to other rhabdoviruses from *Culex* and *Aedes* mosquitoes, sharing low amino acid similarity (less than 53%) with each other. Similarly, *Armigeres* rhabdo-like virus 1 (ARLV1) and *Aedes* rhabdovirus 1 (ARV1) clustered with viruses identified from other mosquito species (Fig. 3B), with the largest amino acid similarities of 72.52% and 48.08% over RdRp (Table 1), respectively. *Culex* rhabdo-like virus 2 (CRLV2) and *Culex* quinquefasciatus rhabdo-like virus 1 (CQRLV1) were related to *Culex* rhabdo-like viruses (Fig. 3B). CQRLV1 shared 94.67% amino acid similarity in RdRp to the closest reference sequence—*Culex pseudovishnui* rhabdo-like virus. Notably, all the five novel *Rhabdoviridae* viruses possessed linear genomes, with typical genome structures comprising 4 to 5 ORFs (Fig. 3B).

One novel *Armigeres* orthomyxo-like virus 1 (ArOLV1) was identified in *Armigeres* mosquitoes and belonged to an unclassified mosquito-associated clade related to



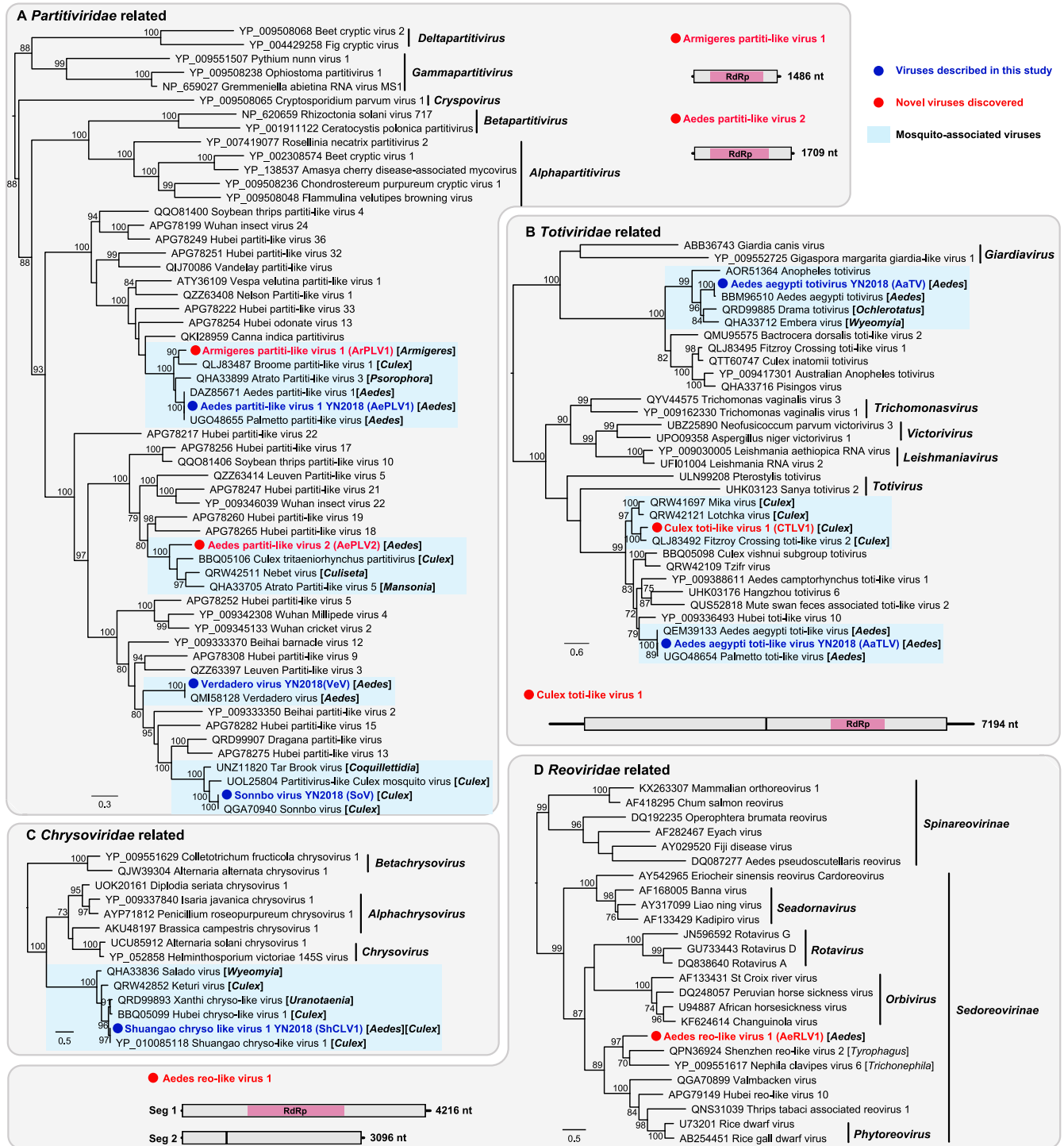


**FIG 2** Evolutionary relationships and genomic features of the double-stranded RNA viruses identified in this study. Viruses identified in this study are marked in red/blue and highlighted with a red/blue solid circle. Mosquito-associated viruses are shaded in the blue box. All phylogenetic trees were midpoint rooted for clarity, and only bootstrap values (>70%) are shown adjacent to the nodes. The diagrams provide the genome information of the newly discovered viruses, including the length of each genomic segment, the number of ORFs and the predicted RdRp protein (shown in the pink box).

the *Orthomyxoviridae* (Fig. 3C). ArOLV1 clustered with Usinis virus isolated from *Aedes* mosquitoes, with an amino acid similarity of 69.27% in the RdRp protein. Although the number of genome segments in the family *Orthomyxoviridae* ranged from 6 to 8, only 5 genome segments were obtained through sequence similarity from our data, including PB1, PB2, PA, nucleoprotein (N), and the glycoprotein (G) genes (Fig. 3C).





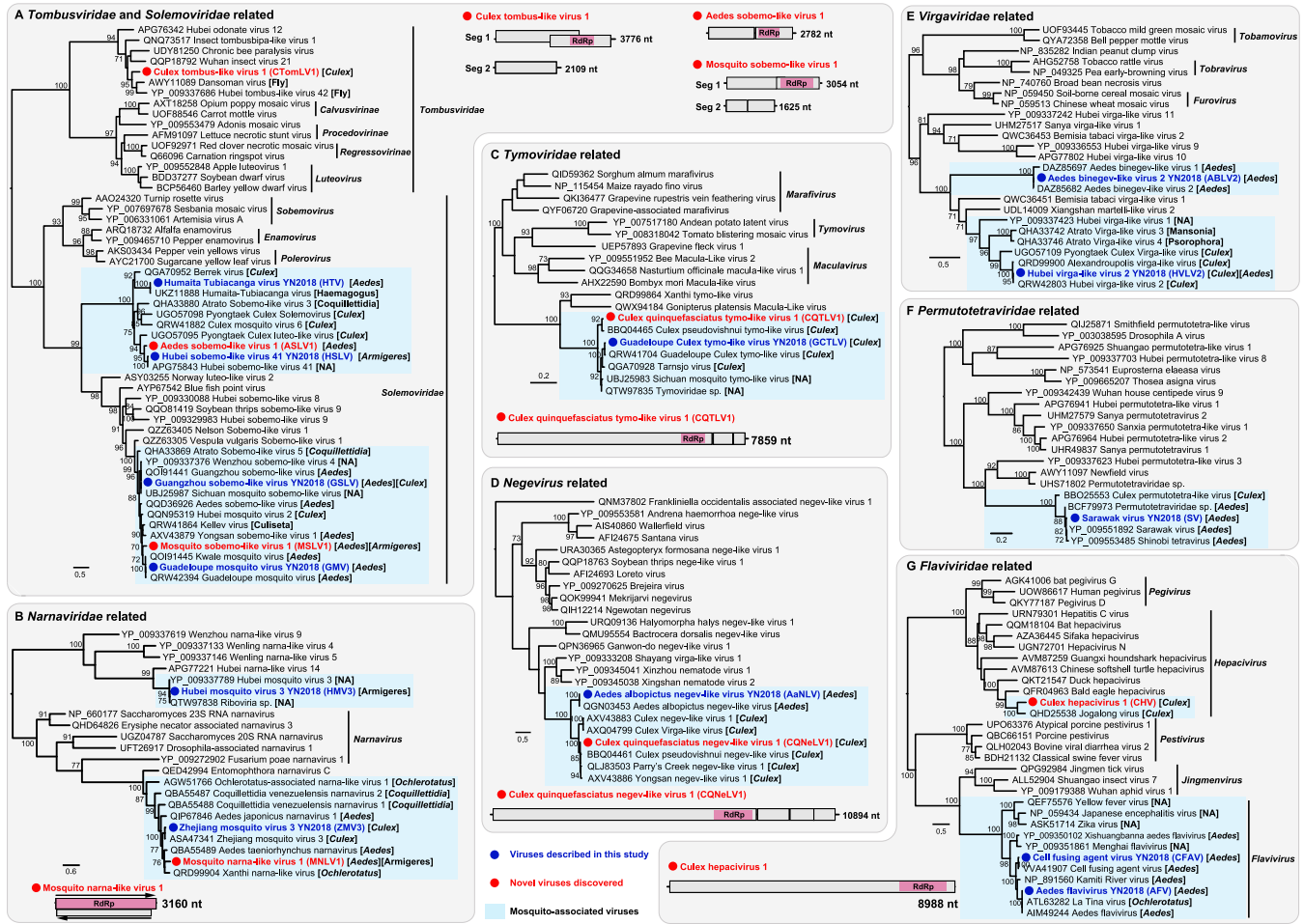


**FIG 4** Evolutionary relationships and genomic features of the positive-sense RNA viruses identified in this study. Viruses identified in this study are marked in red/blue and highlighted with a red/blue solid circle. Mosquito-associated viruses are shaded in the blue box. All phylogenetic trees were midpoint rooted for clarity, and only bootstrap values (>70%) are shown adjacent to the nodes. The diagrams provide the genome information of the newly discovered viruses, including the length of each genomic segment, the number of ORFs, and the predicted RdRp protein (shown in the pink box).

We identified two novel viruses of the family *Solemoviridae*: *Aedes sobemo*-like virus 1 (ASLV1) and *Mosquito sobemo*-like virus 1 (MSLV1), which were related to *Hubei sobemo*-like virus 41, previously identified in mosquitoes from China, and *Guadeloupe* mosquito virus from the Caribbean, respectively (Fig. 4A). ASLV1 and MSLV1 had similar genome structures to their closest relatives and exhibited RdRp amino acid identities of 87.6% and 83.45%, respectively (Table 1). Notably, MSLV1 was identified in both *Aedes* and *Armigeres* mosquitoes (Fig. 4A), showing broader host ranges (host-sharing events) across different mosquito genera.

Another host-sharing event was identified in the novel *Mosquito narna*-like virus 1 (MNLV1), which was also found in both *Aedes* and *Armigeres* mosquitoes (Fig. 4B). MNLV1 was closely related to reference strains identified in *Aedes*, *Culex*, *Coquillettidia*, and *Ochlerotatus* mosquitoes and shared 36.17% amino acid similarity with *Ochlerotatus*-associated *narna*-like virus 2. MNLV1 had the same genome structure as its closest relative, with a dual-coding genome structure: two ORFs cover both the sense and antisense genomes, encoding RdRp and a hypothetical protein (Fig. 4B).

We also identified two novel viruses related to the *Tymoviridae* and *Negev*-like viruses (Fig. 4C and D). *Culex quinquefasciatus* tymo-like virus 1 (CQTLV1) clustered within the clade of mosquito-associated viruses identified in *Culex* mosquitoes (Fig. 4C), sharing 87.01% amino acid similarity with *Culex pseudovishnui* tymo-like virus. Similarly, *Culex quinquefasciatus* negev-like virus 1 (CQNELV1) and *Culex* mosquito-associated negev-like viruses formed a clade and showed 90.05% amino acid similarity with *Parry's Creek* negev-like virus 1 (Fig. 4D).

Of particular note was the identification of a novel hepacivirus, termed *Culex* hepacivirus 1 (CHV1), from a *Culex quinquefasciatus* mosquito library (Fig. 4G). CHV1 was related to a previously described mosquito-associated virus (Jogalong virus [JgV]) (16), which was identified in *Culex annulirostris* mosquitoes from Western Australia, sharing 54.62% amino acid sequence similarity with each other. Notably, CHV1 and JgV clustered within the clade of hepaciviruses associated with avian hosts (Fig. 4G), sharing less than 43% amino acid similarity with its closest relative, Bald eagle hepacivirus (Fig. 4G).

**Factors affecting the structure and abundance of mosquito viromes.** Virus compositions and abundances differed substantially between mosquito species. In general, *Aedes* mosquitoes (both *Ae. aegypti* and *Ae. albopictus*) contained more viruses than *Culex* mosquitoes (Fig. 1C) and also had higher abundance (Fig. 1D). The highest viral richness was found in *Ae. albopictus* mosquitoes, with a median of 9.0 (Fig. 5A), followed by *Ae. aegypti* and *C. quinquefasciatus* mosquitoes, with medians of 7 and 6, respectively (Fig. 5A). Similarly, both the Shannon (Fig. 5B) and Simpson (Fig. 5C) effective indices were the highest in *Ae. albopictus*, followed by *Ae. aegypti*, and the lowest values of the two indices were from *C. quinquefasciatus* (Fig. 5).

Of the 52 viral species discovered, 5 were shared between *Aedes* and *Culex* mosquitoes (Fig. 5D; Table S2), and only 2 were shared between *Aedes* and *Armigeres* species (Fig. 5D). No viruses were shared between *Culex* and *Armigeres* mosquitoes (Fig. 5D). Notably, *Ae. aegypti* shared 14 viruses with *Ae. albopictus*, while *C. quinquefasciatus* shared one virus with other *Culex* species (*Lutzia halifaxii*), although only two viruses were discovered in *L. halifaxii* (Fig. 5D). The clustering of the libraries with similar viromic composition and abundance was further described using  $\beta$ -diversity analysis. Principal-coordinate analysis (PCoA) plots based on the Bray-Curtis distance matrices revealed that samples from the same mosquito species clustered together (adonis;  $R^2 = 0.67$ ,  $P = 0.0002$ ) (Fig. 6A), demonstrating that mosquito species affect virome structure.

The possible association between sampling locations and viral composition and abundance was examined further (Fig. S1) by measuring observed richness (Fig. S1A), the Shannon index (Fig. S1B), and the Simpson index (Fig. S1C). Three locations (D, E, and F) contained only one or two libraries with limited virome diversity. Only location H showed a significant difference from locations B and C, suggesting a potential association between the geographic location and the viromic structure of mosquitoes. In addition, PCoA plots based on the Bray-Curtis distance matrices revealed that samples from different locations did not form distinct clusters (Fig. S1D). Hence, there is no strong evidence for geographic structure in mosquito viromes in this study, and the mosquito collection sites were close to each other in this study.

We further constructed a co-occurrence network among mosquito species based on significant positive correlations (Spearman's  $\rho > 0.6$ ;  $P < 0.05$ ) (Fig. 6B). The network was derived from the relative abundance of each virus, comprising 56 nodes (56 mosquito libraries) and 372 edges. Based on the modularity class, the entire network could be parsed into three major modules, corresponding to the three major mosquito species (Fig. 6B). Notably, nodes were inclined to interact more with nodes within the same module than with nodes of other modules. The co-occurrence patterns clearly illustrated the correlations between the mosquito species and viral abundance; however, the network among sampling locations showed no obvious correlations (Fig. S2).

***Wolbachia* diversity and abundance.** As an endosymbiont bacterium, *Wolbachia* was detected in all libraries in this study, with relatively high abundance (11.72 to 2,899.50 RPM) (Fig. 1D; Table S2). The alignment of *Wolbachia* 16S rRNA sequences showed 87.99 to 100% nucleotide identities to each other, and phylogenetic analyses revealed two major lineages (Fig. 7A): the first comprised all *Wolbachia* sequences obtained from *Ae. aegypti*, while the other contained *Wolbachia* sequences from all five mosquito species. The phylogenetic tree indicated that *Wolbachia* sequences from *Ae. aegypti* had higher genetic diversity, while *Wolbachia* sequences from *Ae. albopictus* and *C. quinquefasciatus* were more genetically homogeneous. Further comparisons of the abundance (RPM) of *Wolbachia* gene sequences across libraries revealed significant differences between *Ae. aegypti*, *Ae. albopictus*, and *C. quinquefasciatus* (Fig. 7B). The highest abundance of *Wolbachia* sequences was observed

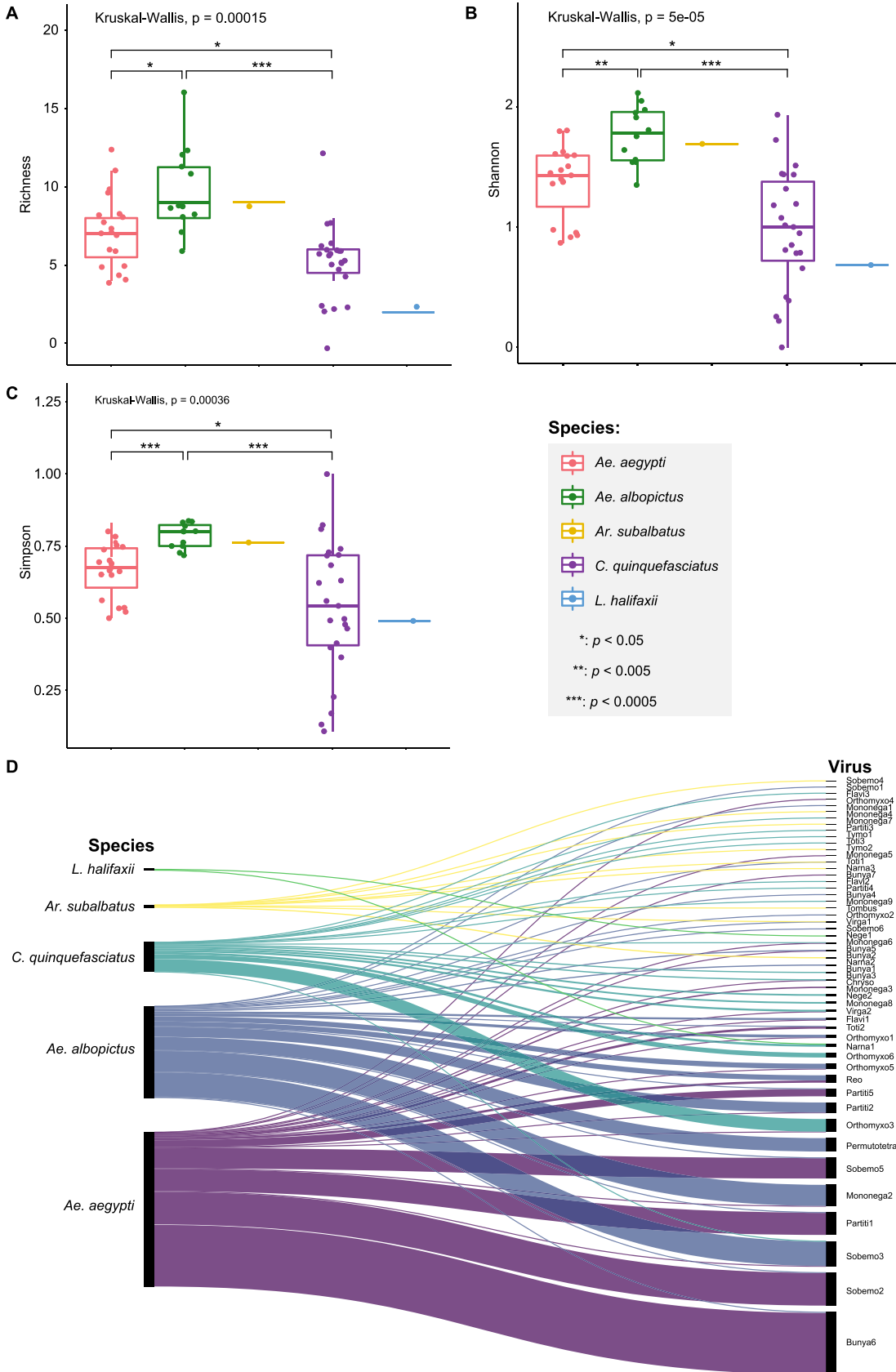


**FIG 5** Comparison of the viral diversity between mosquito species. (A) Virome richness, (B) Shannon index, and (C) Simpson index showing the differences of virome composition between mosquito species; (D) Sankey diagram of the virome compositions of different mosquito species. The thickness of links in the Sankey diagram is proportional to the total abundance (as measured by RPM) of each virus across the samples studied.

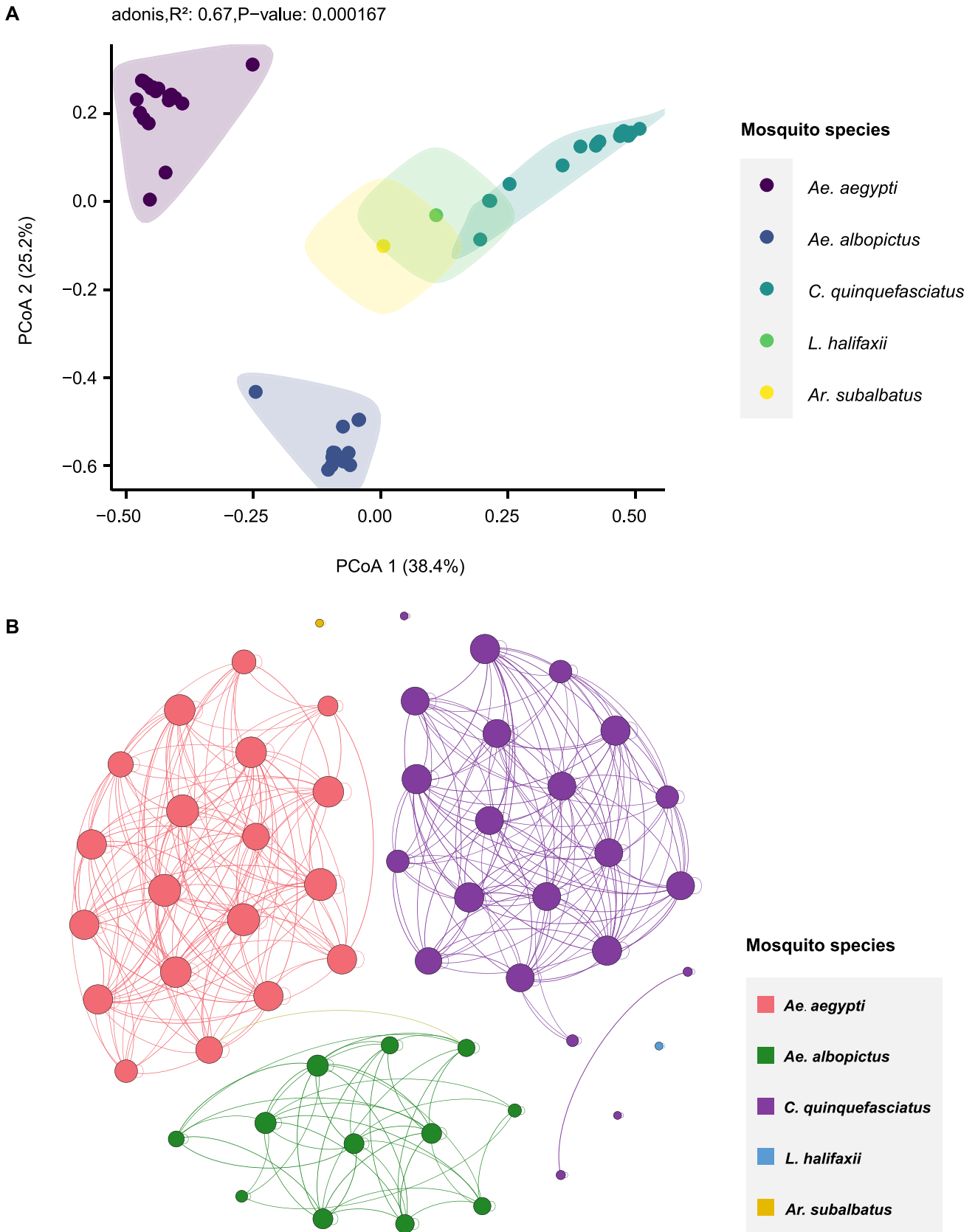


**FIG 6**  $\beta$ -diversity analysis and viral co-occurrence network. (A)  $\beta$ -diversity analysis of the virome composition of different mosquito species; (B) viral co-occurrence network of host taxa. The network was calculated using the relative abundance of each virus across libraries. Each node represents a library. Libraries with a Spearman's correlation greater than 0.6 ( $P < 0.05$ ) are connected by edges. The thickness of each edge is determined according to the correlation coefficient; the size of a node is determined by the degree (number of edge connections). The nodes were colored by mosquito species.

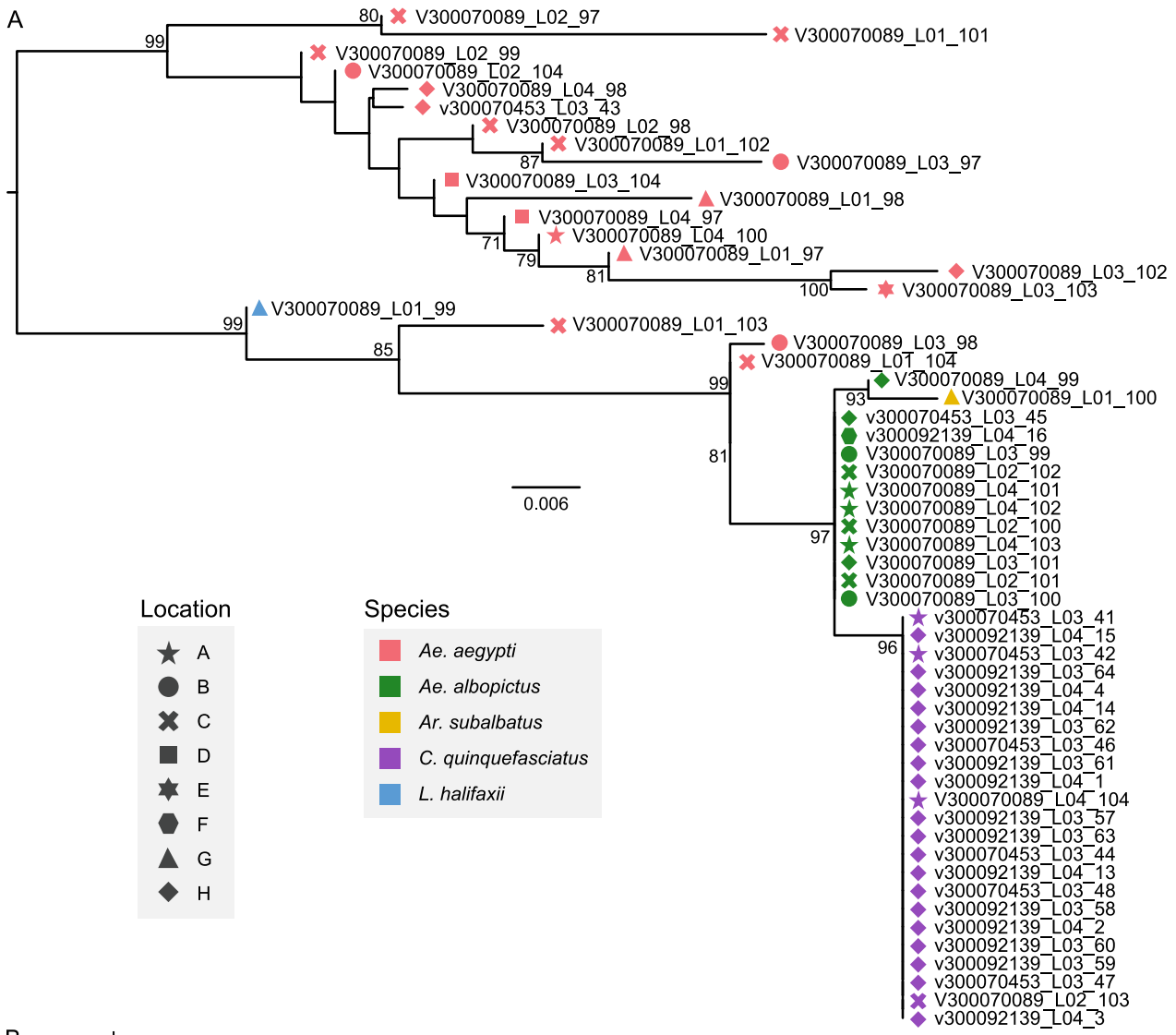


**FIG 7** Genetic diversity and abundance of the *Wolbachia* bacteria. (A) Phylogenetic analysis of the *Wolbachia* bacteria identified in this study performed using the 16S rRNA gene sequences assembled from the sequencing data. Different shapes and colors indicate the sampling location and mosquito species, respectively. (B) Comparison of abundance of *Wolbachia* across five mosquito species.



in *C. quinquefasciatus*, with a median of 1,599.5 RPM, followed by *Ae. albopictus* mosquitoes (median of 977.8), and the lowest abundance was in *Ae. aegypti* mosquitoes, with a median of 25.5 (Fig. 7B).

## DISCUSSION

We present a comprehensive description of the viromes of 991 mosquitoes collected from eight locations in Yunnan Province in southwestern China. Although previous metagenomic studies have revealed numerous novel and highly divergent RNA viruses in mosquitoes, analysis of the transcriptomes of the five mosquito species in the present study has led to the discovery of 52 RNA viruses belonging to 15 viral families and unclassified clades. Notably, 19 viruses were novel, with half sharing 30 to 70% amino acid similarity to their most closely related viruses. One of the most notable discoveries was *Culex quinquefasciatus* bunyavirus 1 (CQBV1), which represented a putative new virus family within the order *Bunyavirales* together with previously described QMV (4). These results underscore the capacity of mosquitoes to harbor a wide diversity of RNA viruses, highlighting the necessity for constant surveillance of potential viral pathogens in these arthropod vectors.

Another key result from our study was that within the *Aedes* mosquito vector species, both *Ae. aegypti* and *Ae. albopictus* harbored significantly greater virus diversity than *Culex* mosquitoes (*Culex quinquefasciatus*). This is in contrast to the observation in a previous report that *Culex* species harbored more viruses at high abundance than *Aedes* mosquitoes (17). The underlying explanation for these contrary results could be due to uneven sample sizes of each mosquito genus. Our results also revealed pronounced differences between the virome structures of *Ae. aegypti* and *Ae. albopictus* mosquitoes: even though there is considerable overlap in the viruses carried by these two *Aedes* mosquitoes, the latter had both higher diversity and viral abundance. These findings were also supported by further statistical and multidimensional scaling analyses and are consistent with prior evidence that different *Aedes* mosquitoes can have significantly different virome compositions (17, 18). Hence, the ecology of mosquito viruses was driven, at least in part, by host taxon, consistent with the predicted narrow host range of insect-specific viruses (6).

In contrast, according to the  $\alpha$ - and  $\beta$ -diversity analyses, the virome structures were relatively homogeneous across different locations. Indeed, some mosquito-specific viruses exhibiting high similarity have been described from different continents (19), indicating that viruses can be transmitted to wide geographical areas through mosquito populations. As all of the sampling sites in the present study were geographically close, larger-scale samplings covering different ecological niches are clearly required for further investigations with respect to the correlation between geographic location and virome structure.

The viruses discovered here expand the host ranges of several mosquito viruses to include additional mosquito species and even genera. For example, Shuangao chryso-like virus 1 YN2018 (ShCLV1), *Culex phasma*-like virus YN2018 (CPLV), and Guangzhou sobemo-like virus YN2018 (GSLV) were identified in both *Aedes* and *Culex* mosquitoes, while Mosquito narna-like virus 1 (MNLV1) was present in both *Aedes* and *Armigeres* mosquitoes with high abundance, suggesting host sharing and the intergeneric transmission of these viruses. However, those viruses that clustered with viruses associated with fungi rather than mosquitoes or arthropods might have been derived from other eukaryotic organisms present in the mosquito microbiome or from fungal infections of the mosquito cuticle.

According to the WHO (20), the most prevalent viral infections are primarily transmitted by *Ae. aegypti*, *Ae. albopictus*, and *C. quinquefasciatus*, including Zika virus fever, dengue, yellow fever, Japanese encephalitis, and West Nile fever. However, surprisingly, none of these known viral pathogens were identified in this study. Interestingly, one virus, CHV, as well as the previously documented JgV (16), clustered with vertebrate-associated hepaciviruses. Phylogenetic analyses of the *Flaviviridae* suggested that both CHV and JgV were likely associated with avian hosts, rather than the mosquito itself. Indeed, through targeting two of the vertebrate mitochondrial genes (*COI* and *Cytb*), JgV was suspected as a contamination from a blood meal taken from a bird host (16). However, we did not find vertebrate mitochondrial genes from the sequencing data. Given the high divergence of these mosquito hepaciviruses, it will be

important to investigate their true natural host, particularly as this may provide valuable information on their evolutionary history. Although analysis of host genes from mosquito sequencing data is highly suggestive of the natural host, viruses detected in the blood of vertebrate species would provide convincing evidence of the real source of the viruses. To this end, more expansive surveillance is required, including a larger collection of mosquitoes and blood samples from vertebrate animals present in the same location.

*Wolbachia* has been documented to provide resistance to the infection with some viruses, such as dengue virus and Zika virus in mosquitoes (21, 22), and hence has been suggested as a potential tool for vector-borne disease control. However, not all *Wolbachia* strains have clear effects in inhibiting virus replication, and *Wolbachia* infection does not protect against all viruses (23, 24). Despite this, little is known about how the ecology of hosts impacts *Wolbachia* diversity. We found *Wolbachia* in all libraries, once again indicating the prevalence of *Wolbachia* in mosquitoes in China (25). However, there was a large discrepancy in the genetic diversity and abundance of *Wolbachia* between different mosquito populations. Specifically, *Wolbachia* in *Ae. aegypti* had high diversity but low abundance, while the converse was seen (low diversity/high abundance) in both *Ae. albopictus* and *C. quinquefasciatus*. These results suggested that mosquito species might also play an important role in *Wolbachia* composition.

We do not believe that the *Wolbachia* sequences identified in *Ae. Aegypti* mosquitoes result from contamination as the *Ae. aegypti* libraries were sequenced on different lanes and sequences within the same lane did not share 100% nucleotide identity. In addition, *Wolbachia*-infected *Ae. Albopictus* mosquitoes, not *Ae. Aegypti*, are being released in a few small independent islands in China (26), and our samples were not collected from these sites. However, *Ae. aegypti* was not thought to naturally harbor *Wolbachia* (27) until recently in some Southeast Asian countries (such as Malaysia, India, the Philippines, and Thailand) as well as the United States (28, 29). None of these studies provide robust evidence that *Ae. aegypti* harbors natural *Wolbachia* infections. The presence of natural *Wolbachia* infections may interfere with compatibility patterns between *Ae. aegypti* mosquitoes and some *Wolbachia* strains (27). Confirmation of a natural infection in these mosquitoes will require significant additional experimental work.

In conclusion, we studied the viral diversity of five mosquito species sampled in different locations in Yunnan Province and highlighted the capacity of mosquitoes to harbor a rich diversity of RNA viruses. The viral compositions varied mainly between different mosquitoes, suggesting host species represents an important factor shaping the virome composition of mosquitoes.

## MATERIALS AND METHODS

**Sample collection.** From October to December 2018, a total of 991 adult mosquitoes were collected using light-traps from eight locations in Jinghong City, Xishuangbanna, Yunnan Province, China (Fig. 1). Mosquito species were initially identified morphologically by experienced field biologists and further confirmed based on sequences of the cytochrome *c* oxidase subunit 1 mitochondrial gene (*COI*). All samples were divided into 56 pools by mosquito species and geographic location and were transported to the laboratory on dry ice.

**Metatranscriptomic sequencing.** Mosquitoes were rinsed three times using RNA- and DNA-free phosphate-buffered saline (PBS) solution (Gibco) before homogenization with steel beads in PBS solution. Total RNA was extracted using TRIzol reagent (Invitrogen). RNA quantity and quality were checked using the Agilent 2100 Bioanalyzer (Agilent). Host rRNA was removed using the MGIEasy rRNA depletion kit according to the manufacturer's instructions, and sequencing libraries were constructed using the MGIEasy mRNA library prep kit. Paired-end (100-bp) sequencing of each RNA library was performed on the BGISEQ-500RS sequencing platform (BGI).

**Data analysis and virus discovery.** A quality assessment of the raw sequencing reads was conducted using the Fastp v.0.19. (30) and Trimmomatic (31) programs, before *de novo* assembly using the Trinity program (32). The assembled contigs were then compared against the nonredundant nucleotide (nt) and protein (nr) databases downloaded from NCBI using blastn (33) and Diamond blastx (34), with cut-off E values of  $1 \times 10^{-10}$  and  $1 \times 10^{-5}$ , respectively. All potential viral contigs were identified and merged into longer viral contigs using Geneious Prime (35). False-positive results due to cross-contamination and index hopping during sequencing were excluded as previously described (36). The relative abundance of the viruses identified was determined by mapping the reads back to the assembled contigs using Bowtie2 v.2.3.3.1 (37) and calculated as the number of reads mapped per million input reads (RPM) using the formula "total mapped reads/total reads  $\times$  1 million." Bowtie2 was used to align the reads to each novel virus genome, and SAMtools (38) was used to compute the percentage of reads mapped and coverage depth. Novel viruses were defined employing the previously

defined criterion such that the translated protein sequence shared less than 90% amino acid similarity in the RNA-dependent RNA polymerase (RdRp) to any previously described viruses (39).

**Phylogenetic analyses.** RdRp sequences of the viruses identified from this study were then aligned with their corresponding homologs in reference viruses using the MAFFT v.7.407 program (40) employing the E-INS-I algorithm, followed by the removal of ambiguously aligned regions using TrimAl v.1.4 (41). Phylogenetic trees were constructed using the maximum likelihood method implemented in IQ-TREE v.1.6.12 (42), employing the best-fit substitution models identified by IQ-TREE.

**Ecological dynamics analysis and network analysis.** Statistical analyses of viral genetic diversity and abundance were performed using the *t* test or Wilcoxon test based on the results of a normal distribution test (Shapiro-Wilk test) in the ggpubr package and were plotted using the ggplot2 package in RStudio v.4.1.2. The observed richness, Shannon index, and Simpson index (i.e.,  $\alpha$  diversity) were estimated for each library using modified Rhea script sets (43) and compared between different mosquitoes using the Kruskal-Wallis rank sum test. Principal-coordinate analysis (PCoA) (i.e.,  $\beta$  diversity) was performed based on the Bray-Curtis dissimilarity matrix using the Vegan package (44). A correlation between two items was considered statistically robust if the Spearman's correlation coefficient ( $\rho$ ) was  $>0.6$  and the *P* value was  $<0.05$ , with the *P* value adjusted with a multiple-testing correction using the Benjamini-Hochberg method (45). All pairwise Spearman's rank correlations between the viral members were calculated using the psych package in RStudio v.4.1.2. Network visualization was conducted on the interactive platform of Gephi (46).

**Identification of *Wolbachia* bacteria.** Bacteria were initially identified in the metatranscriptomic data using MetaPhlan2 (47). The 16S rRNA gene was used to conduct phylogenetic analyses and similarity comparisons for *Wolbachia*. To estimate their relative abundance, sequence reads were mapped to the complete reference genomes (CP031221 [*Wolbachia pipiensis* wAlbB chromosome]) from which the RPM was calculated.

**Ethics statement.** This study was performed in accordance with the institutional and national guidelines for the care and handling of the animals.

**Data availability.** All sequence reads generated in this study have been uploaded into the NCBI Sequence Read Archive (SRA) database under BioProject accession no. PRJNA911492. All novel and known virus genome sequences generated in this study have been deposited in NCBI/GenBank under accession no. OQ067620 to OQ067711.

## SUPPLEMENTAL MATERIAL

Supplemental material is available online only.

**SUPPLEMENTAL FILE 1**, PDF file, 1.1 MB.

**SUPPLEMENTAL FILE 2**, XLSX file, 0.04 MB.

## ACKNOWLEDGMENTS

C. Li was funded by National Natural Science Foundation of China (32200004), the Youth Innovation Team of Shandong Higher Education Institution (2021KJ064), and the Academic Promotion Program of Shandong First Medical University (2019QL006). J. Li was funded by Taishan Scholars Program of Shandong Province. E. C. Holmes was funded by an Australian Research Council Australian Laureate Fellowship (FL170100022).

C. Li and W. Shi designed and supervised the project. J. Wang, J. Liu, J. Zhu, and W. Li collected samples. C. Li, W. Zhu, S. Liu, H. Zhou, and M. Cui performed laboratory work. C. Li, W. Zhu, S. Liu, and J. Li carried out the analyses. C. Li drafted the paper. C. Li, Y. Bi, M. J. Carr, E. C. Holmes, and W. Shi reviewed and edited the manuscript. The authors read and approved the final manuscript.

We declare no conflict of interest.

## REFERENCES

- de Almeida JP, Aguiar ER, Armache JN, Olmo RP, Marques JT. 2021. The virome of vector mosquitoes. *Curr Opin Virol* 49:7–12. <https://doi.org/10.1016/j.coviro.2021.04.002>.
- Xia H, Wang Y, Atoni E, Zhang B, Yuan Z. 2018. Mosquito-associated viruses in China. *Virol Sin* 33:5–20. <https://doi.org/10.1007/s12250-018-0002-9>.
- Ramirez AL, Colmant AMG, Warrilow D, Huang B, Pyke AT, McMahon JL, Meyer DB, Graham RMA, Jennison AV, Ritchie SA, van den Hurk AF. 2020. Metagenomic analysis of the virome of mosquito excreta. *mSphere* 5: e00587-20. <https://doi.org/10.1128/mSphere.00587-20>.
- Li CX, Shi M, Tian JH, Lin XD, Kang YJ, Chen LJ, Qin XC, Xu JG, Holmes EC, Zhang YZ. 2015. Unprecedented genomic diversity of RNA viruses in arthropods reveals the ancestry of negative-sense RNA viruses. *eLife* 4:e05378. <https://doi.org/10.7554/eLife.05378>.
- Bolling BG, Weaver SC, Tesh RB, Vasilakis N. 2015. Insect-specific virus discovery: significance for the arbovirus community. *Viruses* 7:4911–4928. <https://doi.org/10.3390/v7092851>.
- Nouri S, Matsumura EE, Kuo YW, Falk BW. 2018. Insect-specific viruses: from discovery to potential translational applications. *Curr Opin Virol* 33: 33–41. <https://doi.org/10.1016/j.coviro.2018.07.006>.
- Hameed M, Wahaab A, Shan TL, Wang X, Khan S, Di D, Liu XQ, Zhang JJ, Anwar MN, Nawaz M, Li BB, Liu K, Shao DH, Qiu YF, Wei JC, Ma ZY. 2020. A metagenomic analysis of mosquito virome collected from different animal farms at Yunnan-Myanmar border of China. *Front Microbiol* 11:591478. <https://doi.org/10.3389/fmicb.2020.591478>.
- Hassell JM, Newbold T, Dobson AP, Linton YM, Franklins LHV, Zimmerman D, Lohan KMP. 2021. Towards an ecosystem model of infectious disease. *Nat Ecol Evol* 5:907–918. <https://doi.org/10.1038/s41559-021-01454-8>.
- Patterson EI, Villinger J, Muthoni JN, Dobel-Ober L, Hughes GL. 2020. Exploiting insect-specific viruses as a novel strategy to control vector-borne disease. *Curr Opin Insect Sci* 39:50–56. <https://doi.org/10.1016/j.cois.2020.02.005>.
- Ma Y, Li M, Xie L, Gao N, Fan D, Feng K, Yao Y, Zhou Y, Sheng Z, Zhou H, Chen H, An J. 2022. Seroepidemiologic study on convalescent sera from dengue

- fever patients in Jinghong, Yunnan. *Viol Sin* 37:19–29. <https://doi.org/10.1016/j.virs.2021.12.001>.
11. Wu C, Guo XF, Zhao J, Lv Q, Li HB, McNeil EB, Chongsuvivatwong V, Zhou HN. 2017. Behaviors related to mosquito-borne diseases among different ethnic minority groups along the China-Laos border areas. *Int J Environ Res Public Health* 14:1227. <https://doi.org/10.3390/ijerph14101227>.
  12. Zhang FC, Zhao H, Li LH, Jiang T, Hong WX, Wang J, Zhao LZ, Yang HQ, Ma DH, Bai CH, Shan XY, Deng YQ, Qin CF. 2014. Severe dengue outbreak in Yunnan, China, 2013. *Int J Infect Dis* 27:4–6. <https://doi.org/10.1016/j.ijid.2014.03.1392>.
  13. Fang Y, Li XS, Zhang W, Xue JB, Wang JZ, Yin SQ, Li SG, Li XH, Zhang Y. 2021. Molecular epidemiology of mosquito-borne viruses at the China-Myanmar border: discovery of a potential epidemic focus of Japanese encephalitis. *Infect Dis Poverty* 10. <https://doi.org/10.1186/s40249-021-00838-z>.
  14. Li L, Li Y, Lu S, Dong J, Xu H, Zhang Q, Weng R, Yin Y, He R, Fang P, Shi H, Yu Y, Wu J, Liu Z, Hess JR. 2021. Epidemiological survey and screening strategy for dengue virus in blood donors from Yunnan Province. *BMC Infect Dis* 21:104. <https://doi.org/10.1186/s12879-021-05810-8>.
  15. Zhao Y, Li L, Ma D, Luo J, Ma Z, Wang X, Pan Y, Chen J, Xi J, Yang J, Qiu L, Bai C, Jiang L, Shan X, Sun Q. 2016. Molecular characterization and viral origin of the 2015 dengue outbreak in Xishuangbanna, Yunnan, China. *Sci Rep* 6:34444. <https://doi.org/10.1038/srep34444>.
  16. Williams SH, Levy A, Yates RA, Somaweera N, Neville PJ, Nicholson J, Lindsay MDA, Mackenzie JS, Jain K, Imrie A, Smith DW, Lipkin WI. 2020. Discovery of Jogalong virus, a novel hepatitis virus identified in a *Culex annulirostris* (Skuse) mosquito from the Kimberley region of Western Australia. *PLoS One* 15:e0227114. <https://doi.org/10.1371/journal.pone.0227114>.
  17. Shi M, Neville P, Nicholson J, Eden JS, Imrie A, Holmes EC. 2017. High-resolution metatranscriptomics reveals the ecological dynamics of mosquito-associated RNA viruses in Western Australia. *J Virol* 91:e00680-17. <https://doi.org/10.1128/JVI.00680-17>.
  18. Thongsripong P, Chandler JA, Kittayapong P, Wilcox BA, Kapan DD, Bennett SN. 2021. Metagenomic shotgun sequencing reveals host species as an important driver of virome composition in mosquitoes. *Sci Rep* 11:8448. <https://doi.org/10.1038/s41598-021-87122-0>.
  19. Parry R, Asgari S. 2018. *Aedes Anophevirus*: an insect-specific virus distributed worldwide in *Aedes aegypti* mosquitoes that has complex interplays with *Wolbachia* and dengue virus infection in cells. *J Virol* 92:e00224-18. <https://doi.org/10.1128/JVI.00224-18>.
  20. WHO. 2020. Vector-borne diseases. <https://www.who.int/news-room/fact-sheets/detail/vector-borne-diseases>.
  21. Chouin-Carneiro T, Ant TH, Herd C, Louis F, Failloux AB, Sinkins SP. 2020. *Wolbachia* strain wAlbA blocks Zika virus transmission in *Aedes aegypti*. *Med Vet Entomol* 34:116–119. <https://doi.org/10.1111/mve.12384>.
  22. Utarini A, Indriani C, Ahmad RA, Tantowijoyo W, Arguni E, Ansari MR, Supriyati E, Wardana DS, Meitika Y, Ernesia I, Nurhayati I, Prabowo E, Andari B, Green BR, Hodgson L, Cutcher Z, Rances E, Ryan PA, O'Neill SL, Dufault SM, Tanamas SK, Jewell NP, Anders KL, Simmons CP, AWED Study Group. 2021. Efficacy of *Wolbachia*-infected mosquito deployments for the control of dengue. *N Engl J Med* 384:2177–2186. <https://doi.org/10.1056/NEJMoa2030243>.
  23. Ortiz-Baez AS, Shi M, Hoffmann AA, Holmes EC. 2021. RNA virome diversity and *Wolbachia* infection in individual *Drosophila simulans* flies. *J Gen Virol* 102:001639. <https://doi.org/10.1099/jgv.0.001639>.
  24. Wang J, Gou QY, Luo GY, Hou X, Liang G, Shi M. 2022. Total RNA sequencing of *Phlebotomus chinensis* sandflies in China revealed viral, bacterial, and eukaryotic microbes potentially pathogenic to humans. *Emerg Microbes Infect* 11:2080–2092. <https://doi.org/10.1080/22221751.2022.2109516>.
  25. Yang Y, He Y, Zhu G, Zhang J, Gong Z, Huang S, Lu G, Peng Y, Meng Y, Hao X, Wang C, Sun J, Shang S. 2021. Prevalence and molecular characterization of *Wolbachia* in field-collected *Aedes albopictus*, *Anopheles sinensis*, *Armigeres subalbatus*, *Culex pipiens* and *Cx. tritaeniorhynchus* in China. *PLoS Negl Trop Dis* 15:e0009911. <https://doi.org/10.1371/journal.pntd.0009911>.
  26. Zheng B, Yu JS, Li J. 2021. Modeling and analysis of the implementation of the *Wolbachia* incompatible and sterile insect technique for mosquito population suppression. *SIAM J Appl Math* 81:718–740. <https://doi.org/10.1137/20M1368367>.
  27. Ross PA, Callahan AG, Yang Q, Jasper M, Arif MAK, Afizah AN, Nazni WA, Hoffmann AA. 2020. An elusive endosymbiont: does *Wolbachia* occur naturally in *Aedes aegypti*? *Ecol Evol* 10:1581–1591. <https://doi.org/10.1002/ece3.6012>.
  28. Balaji S, Jayachandran S, Prabakaran SR. 2019. Evidence for the natural occurrence of *Wolbachia* in *Aedes aegypti* mosquitoes. *FEMS Microbiol Lett* 366:fnz055. <https://doi.org/10.1093/femsle/fnz055>.
  29. Zhang HD, Gao J, Ma Z, Liu Y, Wang G, Liu Q, Du YT, Xing D, Li CX, Zhao T, Jiang YT, Dong YD, Guo XX, Zhao TY. 2022. *Wolbachia* infection in field-collected *Aedes aegypti* in Yunnan Province, southwestern China. *Front Cell Infect Microbiol* 12:1082809. <https://doi.org/10.3389/fcimb.2022.1082809>.
  30. Chen SF, Zhou YQ, Chen YR, Gu J. 2018. fastp: an ultra-fast all-in-one FASTQ preprocessor. *Bioinformatics* 34:i884–i890. <https://doi.org/10.1093/bioinformatics/bty560>.
  31. Bolger AM, Lohse M, Usadel B. 2014. Trimmomatic: a flexible trimmer for Illumina sequence data. *Bioinformatics* 30:2114–2120. <https://doi.org/10.1093/bioinformatics/btu170>.
  32. Grabherr MG, Haas BJ, Yassour M, Levin JZ, Thompson DA, Amit I, Adiconis X, Fan L, Raychowdhury R, Zeng QD, Chen ZH, Mauceli E, Hacohen N, Gnirke A, Rhind N, di Palma F, Birren BW, Nusbaum C, Lindblad-Toh K, Friedman N, Regev A. 2011. Full-length transcriptome assembly from RNA-Seq data without a reference genome. *Nat Biotechnol* 29:644–652. <https://doi.org/10.1038/nbt.1883>.
  33. Camacho C, Coulouris G, Avagyan V, Ma N, Papadopoulos J, Bealer K, Madden TL. 2009. BLAST plus: architecture and applications. *BMC Bioinformatics* 10:421. <https://doi.org/10.1186/1471-2105-10-421>.
  34. Buchfink B, Xie C, Huson DH. 2015. Fast and sensitive protein alignment using DIAMOND. *Nat Methods* 12:59–60. <https://doi.org/10.1038/nmeth.3176>.
  35. Kearse M, Moir R, Wilson A, Stones-Havas S, Cheung M, Sturrock S, Buxton S, Cooper A, Markowitz S, Duran C, Thierer T, Ashton B, Meintjes P, Drummond A. 2012. Geneious Basic: an integrated and extendable desktop software platform for the organization and analysis of sequence data. *Bioinformatics* 28:1647–1649. <https://doi.org/10.1093/bioinformatics/bts199>.
  36. Mahar JE, Shi M, Hall RN, Strive T, Holmes EC. 2020. Comparative analysis of RNA virome composition in rabbits and associated ectoparasites. *J Virol* 94:e02119-19. <https://doi.org/10.1128/JVI.02119-19>.
  37. Langmead B, Salzberg SL. 2012. Fast gapped-read alignment with Bowtie 2. *Nat Methods* 9:357–359. <https://doi.org/10.1038/nmeth.1923>.
  38. Li H, Handsaker B, Wysoker A, Fennell T, Ruan J, Homer N, Marth G, Abecasis G, Durbin R, Genome Project Data Processing S. 2009. The Sequence Alignment/Map format and SAMtools. *Bioinformatics* 25:2078–2079. <https://doi.org/10.1093/bioinformatics/btp352>.
  39. Edgar RC, Taylor J, Lin V, Altman T, Barbera P, Meleshko D, Lohr D, Novakovsky G, Buchfink B, Al-Shayeb B, Banfield JF, de la Pena M, Korobeynikov A, Chikhi R, Babaian A. 2022. Petabase-scale sequence alignment catalyses viral discovery. *Nature* 602:142–147. <https://doi.org/10.1038/s41586-021-04332-2>.
  40. Katoh K, Standley DM. 2013. MAFFT Multiple Sequence Alignment software version 7: improvements in performance and usability. *Mol Biol Evol* 30:772–780. <https://doi.org/10.1093/molbev/mst010>.
  41. Capella-Gutierrez S, Silla-Martinez JM, Gabaldon T. 2009. trimAl: a tool for automated alignment trimming in large-scale phylogenetic analyses. *Bioinformatics* 25:1972–1973. <https://doi.org/10.1093/bioinformatics/btp348>.
  42. Nguyen LT, Schmidt HA, von Haeseler A, Minh BQ. 2015. IQ-TREE: a fast and effective stochastic algorithm for estimating maximum-likelihood phylogenies. *Mol Biol Evol* 32:268–274. <https://doi.org/10.1093/molbev/msu300>.
  43. Lagkouvardos I, Fischer S, Kumar N, Clavel T. 2017. Rhea: a transparent and modular R pipeline for microbial profiling based on 16S rRNA gene amplicons. *PeerJ* 5:e2836. <https://doi.org/10.7717/peerj.2836>.
  44. Oksanen J, Blanchet F. G, Friendly M, Kindt R, Legendre P, McGinn D, Minchin PR, O'Hara RB, Simpson GL, Solymos P, Stevens MHH, Szoecs E, Wagner H. 2020. vegan: Community Ecology Package. <https://cran.r-project.org/web/packages/vegan/index.html>.
  45. Benjamini Y, Hochberg Y. 1995. Controlling the false discovery rate: a practical and powerful approach to multiple testing. *J R Stat Soc Series B Methodol* 57:289–300. <https://doi.org/10.1111/j.2517-6161.1995.tb02031.x>.
  46. Bastian M, Heymann S, Jacomy M. 2009. Gephi: an open source software for exploring and manipulating networks, p 361–362. *In Proceedings of the Third International AAAI Conference on Weblogs and Social Media*. AAAI, Palo Alto, CA.
  47. Segata N, Waldron L, Ballarini A, Narasimhan V, Jousson O, Huttenhower C. 2012. Metagenomic microbial community profiling using unique clade-specific marker genes. *Nat Methods* 9:811–814. <https://doi.org/10.1038/nmeth.2066>.